Research Square

Preprints are preliminary reports that have not undergone peer review.
They should not be considered conclusive, used to inform clinical practice,
or referenced by the media as validated information.

Hemodynamic and ventilation/perfusion effects of continuous anterior chest compression in acute respiratory distress syndrome

Pascale Labedade

pascale.labedade@aphp.fr

Hôpitaux Universitaires Henri-Mondor

Samuel Tuffet

Centre Hospitalier Saint-Joseph Saint-Luc

Paul Masi

Hôpitaux Universitaires Henri-Mondor

Elsa Moncomble

Hôpitaux Universitaires Henri-Mondor

Mohamed Boujelben

Hopital Saint Camille

Anne-Fleur Haudebourg

Hôpitaux Universitaires Henri-Mondor

François Bagate

Hôpitaux Universitaires Henri-Mondor

Armand Mekontso Dessap

Hôpitaux Universitaires Henri-Mondor

Guillaume Carteaux

Hôpitaux Universitaires Henri-Mondor

Research Article

Keywords: Acute respiratory distress syndrome, Chest loading, ventilation-perfusion matching, overdistension, right heart afterload

Posted Date: July 10th, 2026

DOI: https://doi.org/10.21203/rs.3.rs-10193805/v1

License: This work is licensed under a Creative Commons Attribution 4.0 International License.
Read Full License

Additional Declarations: No competing interests reported.

Hemodynamic and ventilation/perfusion effects of continuous anterior chest compression in acute respiratory distress syndrome

Pascale Labedade [1,2,3] M.D., Samuel Tuffet[2,3,4] M.D., Paul Masi[1,2,3] M.D., Elsa Moncomble[1,2,3] M.D., Mohamed Boujelben[5] M.D., Anne Fleur Haudebourg[1,2,3] M.D., François Bagate[1,2,3] M.D.,PhD, Armand Mekontso Dessap[1,2,3] M.D., Ph.D., Guillaume Carteaux[1,2,3] M.D., Ph.D.

Authors' affiliations:

1. AP-HP, Hôpitaux Universitaires Henri-Mondor, Service de Médecine Intensive Réanimation, 94010, Créteil, France
2. INSERM U955, Institut Mondor de Recherche Biomédicale, Créteil, France
3. Faculté de Santé, Groupe de Recherche Clinique CARMAS, Université Paris Est-Créteil, 94010 Créteil, France
4. Hôpital Saint Joseph Saint Luc, Lyon, France
5. Hôpital St Camille, service de réanimation polyvalente, Bry sur Marne

Correspondence to:

Pascale Labedade, M.D, Centre hospitalier universitaire Henri Mondor, 1 rue Gustave Eiffel, médecine intensive réanimation, 94000, Créteil, France

E-mail : pascale.labedade@aphp.fr

Word count: 2887

ABSTRACT:

Background

In acute respiratory distress syndrome (ARDS), standardized continuous anterior chest compression (CACC) can paradoxically decrease plateau pressure (Pplat) in patients with substantial overdistension ("responders") but not in others ("nonresponders"). We hypothesized that CACC may affect right ventricular (RV) function and ventilation/perfusion (V/Q) matching differently according to the Pplat response.

Objectives

To assess the effects of CACC on RV function and V/Q matching according to the Pplat response in patients with moderate-to-severe ARDS.

Methods

In this prospective, single-center physiological study, 20 patients with moderate-to-severe ARDS were studied at baseline and during CACC (60-80 cmH_2O). RV function was assessed by echocardiography, and V/Q matching by ventilation/perfusion electrical impedance tomography.

Results

At baseline, responders (n=11) had greater overdistension (30% vs 13%, p = 0.013) and wasted ventilation (32% vs 15%, p = 0.021) than nonresponders (n=9). In responders, CACC reduced the tricuspid regurgitation pressure gradient 29 (23; 35) to 21 (18; 29) mmHg; p = 0.004) and improved RV-pulmonary artery coupling (0.42 (0.36; 0.63) to 0.57 (0.43; 0.66); p = 0.008) without affecting cardiac output or central venous pressure; and ventilation of dead-space units tended to decrease (12% to 6%). In nonresponders, CACC raised perfusion of shunt units (2% to 5%, p = 0.02) and lowered PaO_2/FiO_2.

Conclusions

CACC reduced RV afterload and improved RV-pulmonary artery coupling in patients whose Pplat paradoxically decreased (responders), likely by relieving regional overdistension, but worsened V/Q matching by increasing shunt in nonresponders.

Trial registration: ClinicalTrials.gov : NCT05876468, retrospectively registered 28/02/2023.

Key words: Acute respiratory distress syndrome, Chest loading, ventilation-perfusion matching, overdistension, right heart afterload

Introduction

Acute respiratory distress syndrome (ARDS) is characterized by diffuse alveolar injury leading to heterogeneous lung aeration (1). Typically, non-aerated posterior regions coexist with well-aerated anterior regions (2), a distribution resulting from gravitational forces, chest wall compliance inhomogeneity, and the weight of heart and edematous lung (3). This heterogeneity contributes to ventilation/perfusion (V/Q) mismatch, with perfusion of collapsed lung regions (shunting) and ventilation of non-perfused zones (dead space), both of which impair gas exchange and independently predict mortality (4–9).

In addition, pulmonary perfusion may be impaired by several mechanisms, including hypoxic (10) and hypercapnia-induced (11) vasoconstriction, micro- and macrovascular thrombosis (12), and extravascular compression of vessels by edema and alveolar distention (13), all of which exacerbate V/Q mismatch. Among these mechanisms, overdistension, through compression of intra-alveolar vessels within overdistended alveoli (14), is likely a be a key contributor. It has been implicated in both ventilator-induced lung injury (VILI) (15) and pulmonary vascular dysfunction, leading to increased dead space and elevated right ventricular afterload (13). Although previous studies have suggested that this afterload effect may be more pronounced in patients with limited recruitability (11,16), a direct association with the degree of overdistension per se remains unproven.

Recent evidence suggests that chest wall loading, through continuous anterior chest compression (CACC) (17–22) or abdominal compression (22–24), may paradoxically improve respiratory system compliance in some patients with ARDS. In such cases, reducing end-expiratory lung volume (EELV) via external compression may shift overdistended lung regions toward a more compliant portion of the pressure-volume curve, thereby improving respiratory mechanics (18,19). Recent findings also indicate that the change in plateau pressure (Pplat) induced by CACC is correlated with the extent of lung overdistension during protective ventilation (25). However, the effects of CACC on pulmonary perfusion remain unknown.

We hypothesized that the hemodynamic effects of CACC may depend on underlying respiratory mechanics and that CACC could improve right ventricular loading conditions in patients with overdistended lung regions.

The aim of this study was to evaluate the effects of CACC on right ventricular function, respiratory mechanics, gas exchange, and V/Q ratios according to the Pplat response to CACC.

Methods

Design

This was a prospective, single-center physiological study conducted between February 2023 and May 2024 in patients with moderate-to-severe ARDS. The study protocol was approved by the French Ethics Committee *"Comité de Protection des Personnes Sud-Est I"* (2022-A02707-36). Written informed consent was obtained from the patient's legally authorized representative prior to inclusion. The research was retrospectively registered the 28/02/2023 on ClinicalTrials.gov (NCT03919331).

Patients

Inclusion criteria were: age ≥ 18 years, moderate-to-severe ARDS according to the Berlin definition (26), and passive ventilation with neuromuscular blockade (i.e., absence of inspiratory effort). Exclusion criteria were extracorporeal membrane oxygenation, pneumothorax, chest trauma within the past 3 months, uncontrolled shock (defined as norepinephrine > 5 mg/h), pregnancy, legal incapacity, absence of national health insurance coverage, and conditions precluding the use or interpretation of electrical impedance tomography (EIT), including pacemakers, implantable defibrillators, continuous renal replacement therapy, or thoracic skin lesions.

Study Protocol

The study consisted of two consecutive steps: baseline and CACC application. Respiratory mechanics, EIT-based ventilation and perfusion analysis, arterial and central venous blood gases, echocardiography, and hemodynamics parameters were assessed at both phases. All measurements were performed with the patient in a semi-recumbent position at 30°.

At baseline, patients were ventilated using volume assist-control ventilation, with a tidal volume set at 6 ml/kg of predicted body weight (PBW). Positive end-expiratory pressure (PEEP) set by clinician. CACC was performed

by compressing a 500 mL saline bag positioned over the patient's sternum. The pressure within the bag was monitored on the patient's bedside monitor using a standard pressure transducer, allowing titration of the applied compression to 60–80 cmH_2O (25). Data collection started after a minimum of 10 minutes of CACC application. The total duration of CACC application was approximately 30 minutes. At enrollment, demographic and clinical data were collected, including sex, age, body mass index (BMI), Sequential Organ Failure Assessment (SOFA) score (27) and Simplified Acute Physiology Score II (SAPS II) (28).. Clinical follow-up data included duration of ventilation, ICU length-of-stay, ICU mortality, and ventilator-free days at day 28. Details regarding respiratory data acquisition, EIT analysis and echocardiographic measurements are provided in the online supplementary material.

Respiratory mechanics

At baseline, airway opening pressure (AOP) was determined during low-flow insufflation at a PEEP of 5 cmH_2O, as previously described (29). The recruitment-to-inflation (R/I) ratio was assessed using a single-breath maneuver involving an abrupt PEEP decrease from 15 to 5 cmH_2O (or AOP), as reported elsewhere (30). The plateau pressure was measured both without CACC and during its application using a 0.5-second end-inspiratory occlusion. Patients in whom plateau pressure decreased during chest compression were considered "responders", whereas those in whom plateau pressure increased or was stable were classified as "nonresponders". An arterial and venous blood gas was collected at baseline and during CACC application.

Hemodynamic Parameters

Both transthoracic and transesophageal echocardiography were performed at baseline and during CACC application using a General Electric® VIVID S70system. All echocardiographic images were interpreted offline by two investigators: the clinician who performed the data acquisition and one experienced investigator (PM or FB) blinded of the experimental step and responder status. In cases where differences greater than 10% were observed, cardiac images were reviewed until consensus was found. The effect of CACC on right ventricular afterload was assessed using the ratio of tricuspid annular plane systolic excursion (TAPSE) to right ventricle systolic pressure (RVSP), chosen as a

126 noninvasive surrogate of right ventricle-pulmonary artery coupling, as previously described (31–33).
127 Other parameters of left and right ventricular systolic and diastolic function are detailed in the Online
128 Supplementary Material.

129 EIT Ventilation and Perfusion Assessment

130 EIT data were acquired using the Enlight-1800 system (Timpel, Brazil). Impedance variations, airflow,
131 and airway pressure measurements were recorded at a frequency of 50 Hz using a 32-electrode belt
132 (positioned at the 4^{th}-5^{th} intercostal space) and a proximal pneumotachograph.

133 At baseline, decremental PEEP trial was performed from 24 cmH_2O (or lower, depending on
134 hemodynamics tolerance and with a safety limit of maximum plateau pressure at 39 cmH_2O) to 4-6
135 cmH_2O, in steps of 2 cmH_2O with a duration 30 second. EIT data were processed using dedicated
136 software (Timpel: software in Labview). The percentage of overdistention and collapse was
137 calculated as previously described by Costa's "overdistension/ Collapse" method (34).

138 Regional lung perfusion was assessed using EIT by injecting a 10-ml bolus of 7.5% hypertonic saline
139 through a central venous jugular catheter during a 10 to 20-second apnea. Perfusion distribution was
140 assessed using a first-pass dilution kinetic model (35). Ventilation and perfusion maps were
141 reconstructed offline using dedicated LabVIEW-based software.

142 Global and Regional Analysis of V/Q Mismatch

143 Ventilation and perfusion maps were generated and analyzed to assess the V/Q ratio across
144 individual pixels, following a method described in the Online Supplementary Material. Pixels were
145 then classified into five categories according to their V/Q classes as previously described (36) : shunt
146 pixels (V/Q ratio < 0.1), low V/Q ratio pixels (V/Q ratio 0.1–0.5), normal V/Q ratio pixels (V/Q ratio
147 0.5–2), high V/Q ratio pixels (V/Q ratio 2–10), and dead space pixels (V/Q ratio > 10) (36). Wasted
148 ventilation and wasted perfusion were computed as previously described (37) :

- Wasted ventilation $= \sum_{i=1}^{n} \left(\log \left(\frac{\dot{V}}{Q} \right)_i * Vt_i \right)$, where n is the number of pixels in the functional EIT image within each ROI, including only units with V/Q ratio >1
- Wasted perfusion $= \sum_{i=1}^{n} \left(\log \left(\frac{\dot{V}}{Q} \right)_i * Q_i \right)$, where n is the number of pixels in the functional EIT image each ROI, including only units with V/Q ratio <1

Statistical Analysis

Results are expressed as median [25th-75th percentile] for quantitative data and as number (percentage) for qualitative data. Comparisons between variables assessed during the two study phases (i.e., baseline vs CACC) and between responders and non -responders at baseline, were performed using a Wilcoxon test, or a Mann Whitney test, respectively. Qualitative variables were compared using Fisher's exact test. A two-tailed p-value of less than 0.05 was considered statistically significant. Correlation between variables of interest was assessed using simple linear regression, with statistical significance defined as a two-sided p-value < 0.05. All statistical analyses were conducted using Prism (GraphPad Prism v.10, La Jolla, CA, USA).

Results

Patients, respiratory mechanics and blood gases

We included 20 patients with moderate-to-severe ARDS, distributed between responders (n=11) and nonresponders (n=9). Patient characteristics are presented in Table 1. Although ventilator settings did not differ between responders and nonresponders, baseline AOP and the R/I ratio were significantly lower in the responder group. In responders, the decrease in Pplat induced by CACC was associated with a concurrent reduction in driving pressure and an improvement in respiratory system compliance. CACC was associated with a significant decrease in PaO_2/FiO_2 ratio in nonresponders, whereas $PaCO_2$ remained unchanged regardless of response (Table 2).

Hemodynamics and echocardiographic parameters

Hemodynamic and echocardiographic parameters are summarized in **Table 2 and Table 3**, respectively. Baseline hemodynamic and echocardiographic parameters were similar between responders and nonresponders. In responders, CACC reduced the tricuspid regurgitation pressure gradient from 29 (23; 35) mmHg to 21 (18; 29) mmHg (p = 0.004) and improved right ventriculo-arterial coupling from 0.42 (0.36; 0.63) to 0.57 (0.43; 0.66) (p = 0.008), without affecting cardiac output (**Figure 1**). All other indices of microcirculation, right and left ventricular systolic and diastolic function remained unchanged in both groups.

Ventilation, perfusion and their matching

Tables 4 and Figure 2 present the effects of CACC on ventilation and perfusion distributions, while regional details are depicted in **figure 3**, Online Supplement **Table E1 and Figure E1**. At baseline, ventilation parameters were similar between groups. CACC induced a marked reduction in end-expiratory lung volume and impedance across all regions and in all groups (**Table 4 and E2**). This reduction was significantly higher in anterior zone than posterior (**Table E2**). In responders, CACC

significantly improved regional compliance, with the most pronounced effect observed in anterior lung regions, leading to a redistribution of ventilation toward these regions (**Figure 3**) and a significant reduction of the center of ventilation **(Table 4)**.

At baseline, responders exhibited significantly greater overdistension and wasted ventilation than nonresponders (**Table 4, Figure E2**). Overdistension was strongly correlated with wasted ventilation ($r = 0.78$, $p = 0.0006$; **Figure 4**). Among responders, CACC tended to decrease ventilation directed toward dead-space units (**Table 4, Figure 2**). CACC also increased perfusion to shunt and low V/Q units in nonresponders, resulting in greater wasted perfusion (**Table 4, Figure 2, Figure E2**).

Discussion

In this physiological study including 20 patients with moderate-to-severe ARDS, CACC elicited distinct respiratory and hemodynamic responses according to patients' physiological profiles. Despite similar ventilator settings, responders had lower baseline AOP and R/I ratio and greater regional overdistension, suggesting limited lung recruitability. In these patients, CACC improved right ventriculo-arterial coupling and tended to redistribute ventilation in non-dependent regions from dead-space units toward higher V/Q units. In contrast, nonresponders experienced worsening oxygenation and a significant increase in perfusion to low V/Q and shunt units, with no improvement in hemodynamics. These findings suggest that CACC may improve ventilation, perfusion, and right ventricular afterload specifically in patients with low recruitability and regional overdistension.

Physiological effect of CACC on lung mechanics and heart-lung interactions

In responders, CACC improved respiratory system compliance, particularly in anterior lung regions, while reducing EELV. These findings suggest that the improvement in compliance was primarily driven by a reduction in overdistension, which was more pronounced in responders at baseline. This interpretation is supported by the greater compliance gain observed in anterior regions, which are more susceptible to overdistension and West zone I conditions. These findings are consistent with previous studies in patients with C-ARDS (19,21,24,38,39). Pacchiarini et al. further supported this hypothesis by showing that the reduction in EELI, a surrogate for EELV, induced by abdominal compression improved respiratory mechanics only when overdistension predominated over collapse at a given PEEP (22). Reducing end-tidal overdistension may also influence the anteroposterior distribution of ventilation, as suggested by the reduction in COV, thereby contributing to increased ventilation of high V/Q units.

Concomitantly with these respiratory system mechanics changes, responders exhibited a significant reduction in tricuspid regurgitation pressure gradient and an improved RV-pulmonary artery coupling. Inspiratory inflation during mechanical ventilation is known to increase end-inspiratory stress (40,41), and pulmonary vascular resistance may increase in patients with ARDS (42), notably through compression of intra-alveolar pulmonary vessel by overdistended alveoli.

As previously reported (22), responders exhibited greater overdistension at baseline. As discussed above, the improvement in regional compliance, particularly in anterior regions, was likely driven by a reduction in overdistension. Previous studies have shown that strategies aimed at limiting overdistension, such as lowering tidal volume or airway pressure, can decrease RV afterload and improve RV-pulmonary artery coupling (41,43). The marked decrease in the tricuspid regurgitation pressure gradient and the improvement in RV-pulmonary artery coupling, occurring without changes in cardiac output or central venous pressure, may therefore be explained by enhanced regional lung compliance, particularly in anterior regions, secondary to reduced alveolar overdistension. This finding is consistent with previous studies showing that the lowest RV outflow impedance is achieved at the PEEP level associated with optimal respiratory system compliance (44).

CACC decreases chest wall compliance and increases pleural pressure. Elevated pleural pressure may increase right atrial pressure, potentially reducing venous return, decreasing RV preload, and impairing cardiac output (45). However, in the present study, CVP and cardiac output remained stable regardless of response status, indicating that CACC was hemodynamically well tolerated.

Physiological effect of CACC on V/Q matching

At baseline, responders exhibited significantly greater ventilation reaching dead-space units and greater overdistension than nonresponders, with no difference in cardiac output. Moreover, wasted ventilation and overdistension were significantly correlated. This phenomenon may be attributed to

an increase in alveolar dead space resulting from compression of intra-alveolar pulmonary vessels by overdistended alveoli, which remain well-ventilated but poorly or non-perfused. These results are consistent with previous studies showing that increased overdistension, induced for instance by increasing PEEP or tidal volume, is accompanied by an increase in alveolar dead space (46,47). By mitigating overdistension, CACC shifted ventilation from dead-space units toward high V/Q units, particularly in anterior regions. This may explain why $PaCO_2$ and end-tidal CO_2 remained stable. Previous studies in patients with C-ARDS and severely impaired compliance, who are more prone to overdistension, have reported reductions in alveolar dead space with similar interventions (20,48).

In nonresponders, CACC tended to increase the fraction of ventilation reaching dead-space units. Unlike in responders, the anteroposterior distribution of ventilation was not modified by CACC in this group. In these patients, the reduction in EELV did not appear to produce the beneficial effects on overdistension observed in responders, which may explain the increase in dead-space ventilation. In a previous series of patients with C-ARDS and higher baseline respiratory system compliance, chest compression worsened driving pressure and was associated with a trend toward increased alveolar dead space (20). In nonresponders, CACC also increased the proportion of perfusion distributed to low V/Q and shunt units, resulting in a significant increase in wasted perfusion. Consequently, the PaO_2/FiO_2 ratio significantly decreased in this group during CACC application.

Unlike prone positioning, which reduces shunt in dorsal regions (36,49), CACC did not appear to facilitate alveolar recruitment. Indeed, all patients, regardless of response status, experienced a reduction in EELV, which was more pronounced in anterior regions. This observation is consistent with findings from other studies on C-ARDS (17,18). It likely explains why CACC does not improve oxygenation and may even worsen it in nonresponders.

Limitations

Our study has several limitations. First, this was a single-center study with a relatively small sample size, and the limited number of patients in each subgroup reduced its statistical power. In particular, in the nonresponder group, the tricuspid regurgitation pressure gradient could be measured during CACC in only five patients, precluding any firm conclusion regarding the effect of CACC on the right ventricle. Larger studies are needed to confirm these results, particularly in well-defined populations of responders. Second, we did not use esophageal catheters to measure transpulmonary pressure and therefore could not directly compare lung stress with and without CACC. However, based on the available literature, CACC has been shown to reduce end-inspiratory transpulmonary pressure in patients with C-ARDS and low compliance (18,22). Third, the duration of the CACC application was standardized but arbitrarily defined. Longer application periods might have yielded different results. Bastia et al. (18) reported a slight increase in driving pressure over time compared with baseline, although it remained below initial values. Fourth, the intervention steps in this study were not randomized, introducing potential bias. Finally, for the assessment of alveolar ventilation, we used a fixed proportion of anatomical dead space, as previously described (36,50). Although this method has limitations, recent studies suggest that electrical impedance tomography can adequately track trends in VD/VT compared with gold-standard methods (51), supporting the reliability of our approach.

Conclusion

The effects of CACC depended on the patient's physiological profile, namely responder versus nonresponder status. CACC appeared to improve right ventricle-pulmonary artery coupling only in overdistended patients (responders), probably by limiting regional end-tidal overdistension and reducing right ventricular afterload. In contrast, CACC worsened V/Q matching in nonresponders, particularly by increasing shunt. Overall, CACC was hemodynamically well tolerated. Further studies involving larger cohorts of patients with ARDS who respond to CACC are needed to evaluate the potential protective effect of CACC on right ventricular injury.

289

Abbreviations:

AOP: Airway opening pressure

ARDS: Acute respiratory distress syndrome

BMI: Body mass index (BMI)

CACC: Continuous anterior chest compression

CO: cardiac output

CoV: Center of ventilation (CoV)

C_{RS}: Respiratory system compliance

DP_{RS}: Driving pressure of the respiratory system

EELI: End-expiratory lung impedance

EELV: End-Expiratory Lung Volume

EIT: Electrical impedance tomography

GIi: Global inhomogeneity index

PBW: Predicted body weight

P_{pic} : Peak inspiratory pressure

PEEP: Positive end expiratory pressure

$PEEP_t$: total PEEP

P_{plat}: Plateau pressure

Q_c: cardiac output

R/I ratio: Recruitment to inflation ratio

RV : Right ventricle

SpO_2: pulsed Oxygen saturation

VILI: ventilator-induced lung injury

Vt: tidal volume

VTI: velocity time integral

Vte: expired tidal volume

ΔZ: Regional variations in impedance

Declarations:

Ethics approval and consent to participate:

This study was set in compliance with Helsinki Declaration and was approved by the French Ethics Committee "Comité de Protection des Personnes Sud-Est I" (2022-A02707-36). Written informed consent was obtained from the patient's legally authorized representative prior to inclusion.

Consent for publication

Not applicable.

Trial registration:

NCT05876468, retrospectively registered 28/02/2023.

Data availability

The datasets used and/or analysed during the current study are available from

the corresponding author on reasonable request

Fundings: No funding source

Author's contributions:

PL was involved in study design, data collection, data analysis, data interpretation and writing. ST was involved in data collection, data interpretation and writing. PM was involved in data analysis, data interpretation. EM was involved in data collection, data interpretation and writing. MB was involved in data collection, and writing. AF-H was involved in data collection and writing. FB was involved in data collection, and writing, AMD was involved in data interpretation and writing, GC was involved in study design, data analysis, data interpretation and writing. All authors helped to revise the draft of the manuscript. All authors read and approved the final manuscript

Acknowledgement: The authors thank Glasiele Alcala and Marcus Victor for their technical support.

Competing interests: the authors declare no competing interests

References:

1. Gattinoni L, Pesenti A. The concept of "baby lung". Intensive Care Med. juin 2005;31(6):776-84. doi:10.1007/s00134-005-2627-z

2. Gattinoni L, Marini JJ, Pesenti A, Quintel M, Mancebo J, Brochard L. The « baby lung » became an adult. Intensive Care Med. mai 2016;42(5):663-73. doi:10.1007/s00134-015-4200-8

3. Guérin C, Albert RK, Beitler J, Gattinoni L, Jaber S, Marini JJ, et al. Prone position in ARDS patients: why, when, how and for whom. Intensive Care Med. déc 2020;46(12):2385-96. doi:10.1007/s00134-020-06306-w

4. Nuckton TJ, Pittet JF. Pulmonary Dead-Space Fraction as a Risk Factor for Death in the Acute Respiratory Distress Syndrome. The New England Journal of Medicine. 2002.

5. Siddiki H, Kojicic M, Li G, Yilmaz M, Thompson TB, Hubmayr RD, et al. Bedside quantification of dead-space fraction using routine clinical data in patients with acute lung injury: secondary analysis of two prospective trials. Crit Care. 29 juill 2010;14(4):R141. doi:10.1186/cc9206

6. Cepkova M, Kapur V, Ren X, Quinn T, Zhuo H, Foster E, et al. Pulmonary Dead Space Fraction and Pulmonary Artery Systolic Pressure as Early Predictors of Clinical Outcome in Acute Lung Injury. Chest. sept 2007;132(3):836-42. doi:10.1378/chest.07-0409

7. Claude G, Jean R, Jean-Christophe R, Pascal B, Arnaud G, Thierry B, et al. Prone Positioning in Severe Acute Respiratory Distress Syndrome. n engl j med. 2013;10.

8. Briel M, Meade M, Mercat A, Brower RG, Talmor D, Walter SD, et al. Higher vs Lower Positive End-Expiratory Pressure in Patients With Acute Lung Injury and Acute Respiratory Distress Syndrome: Systematic Review and Meta-analysis. JAMA. 3 mars 2010;303(9):865. doi:10.1001/jama.2010.218

9. Spinelli E, Kircher M, Stender B, Ottaviani I, Basile MC, Marongiu I, et al. Unmatched ventilation and perfusion measured by electrical impedance tomography predicts the outcome of ARDS. Crit Care. déc 2021;25(1):192. doi:10.1186/s13054-021-03615-4

10. Brimioulle S, Julien V, Gust R, Kozlowski JK, Naeije R, Schuster DP. Importance of hypoxic vasoconstriction in maintaining oxygenation during acute lung injury: Critical Care Medicine. avr 2002;30(4):874-80. doi:10.1097/00003246-200204000-00027

11. Mekontso Dessap A, Charron C, Devaquet J, Aboab J, Jardin F, Brochard L, et al. Impact of acute hypercapnia and augmented positive end-expiratory pressure on right ventricle function in severe acute respiratory distress syndrome. Intensive Care Med. nov 2009;35(11):1850-8. doi:10.1007/s00134-009-1569-2 PubMed PMID: 19652953; PubMed Central PMCID: PMC3206087.

12. Cavaleiro P, Masi P, Bagate F, d'Humières T, Mekontso Dessap A. Acute cor pulmonale in Covid-19 related acute respiratory distress syndrome. Crit Care. déc 2021;25(1):346. doi:10.1186/s13054-021-03756-6

13. Mekontso Dessap A, Boissier F, Charron C, Bégot E, Repessé X, Legras A, et al. Acute cor pulmonale during protective ventilation for acute respiratory distress syndrome: prevalence, predictors, and clinical impact. Intensive Care Med. mai 2016;42(5):862-70. doi:10.1007/s00134-015-4141-2 PubMed PMID: 26650055.

14. Mekontso Dessap A, Vieillard-Baron A. Scrutinizing the Mechanisms of West Non-Zone 3 Conditions during Tidal Ventilation. Am J Respir Crit Care Med. 2022;205:1262-5. Located at: Pubmed; 35320065. doi:10.1164/rccm.202202-0298ED

15. Slutsky AS, Ranieri VM. Ventilator-Induced Lung Injury. N Engl J Med. 28 nov 2013;369(22):2126-36. doi:10.1056/NEJMra1208707

16. Cappio Borlino S, Hagry J, Lai C, Rocca E, Fouqué G, Rosalba D, et al. The Effect of Positive End-Expiratory Pressure on Pulmonary Vascular Resistance Depends on Lung Recruitability in Patients with Acute Respiratory Distress Syndrome. Am J Respir Crit Care Med. 1 oct 2024;210(7):900-7. doi:10.1164/rccm.202402-0383OC PubMed PMID: 38924520.

17. Rezoagli E, Bastia L, Grassi A, Chieregato A, Langer T, Grasselli G, et al. Paradoxical Effect of Chest Wall Compression on Respiratory System Compliance. Chest. oct 2021;160(4):1335-9. doi:10.1016/j.chest.2021.05.057

18. Bastia L, Rezoagli E, Guarnieri M, Engelberts D, Forlini C, Marrazzo F, et al. External chest-wall compression in prolonged COVID-19 ARDS with low-compliance: a physiological study. Ann Intensive Care. déc 2022;12(1):35. doi:10.1186/s13613-022-01008-6

19. Carteaux G. Potential protective effects of continuous anterior chest compression in the acute respiratory distress syndrome: physiology of an illustrative case. 2021;4.

20. Umbrello M, Lassola S, Sanna A, Pace R, Magnoni S, Miori S. Chest wall loading during supine and prone position in patients with COVID-19 ARDS: effects on respiratory mechanics and gas exchange. Crit Care. 13 sept 2022;26(1):277. doi:10.1186/s13054-022-04141-7

21. Selickman J, Tawfik P, Crooke PS, Dries DJ, Shelver J, Gattinoni L, et al. Paradoxical response to chest wall loading predicts a favorable mechanical response to reduction in tidal volume or PEEP. Crit Care. déc 2022;26(1):201. doi:10.1186/s13054-022-04073-2

22. Pacchiarini G, Pettenuzzo T, Zarantonello F, Sella N, Lumetti G, Boscolo A, et al. The “mechanical paradox” unveiled: a physiological study. Crit Care. 16 mai 2025;29(1). doi:10.1186/s13054-025-05385-9

23. Stavi D, Goffi A, Al Shalabi M, Piraino T, Chen L, Jackson R, et al. The Pressure Paradox: Abdominal Compression to Detect Lung Hyperinflation in COVID-19 Acute Respiratory Distress Syndrome. Am J Respir Crit Care Med. 15 janv 2022;205(2):245-7. doi:10.1164/rccm.202104-1062IM

24. Kummer RL, Shapiro RS, Marini JJ, Huelster JS, Leatherman JW. Paradoxically Improved Respiratory Compliance With Abdominal Compression in COVID-19 ARDS. Chest. nov 2021;160(5):1739-42. doi:10.1016/j.chest.2021.05.012

25. Moncomble E, Tuffet S, Boujelben M, Gendreau S, Labedade P, Haudebourg AF, et al. Paradoxical Response to Standardized Chest Loading May Unveil Occult Overdistension During Protective Ventilation. 2023.

26. Acute Respiratory Distress Syndrome: The Berlin Definition. JAMA. 20 juin 2012;307(23). doi:10.1001/jama.2012.5669

27. Vincent JL, Moreno R, Takala J, Willatts S, De Mendonça A, Bruining H, et al. The SOFA (Sepsis-related Organ Failure Assessment) score to describe organ dysfunction/failure: On behalf of the Working Group on Sepsis-Related Problems of the European Society of Intensive Care Medicine (see contributors to the project in the appendix). Intensive Care Med. juill 1996;22(7):707-10. doi:10.1007/BF01709751

28. Gall J. SIMPLIFIED ACUTE PHYSIOLOGICAL SCORE FOR INTENSIVE CARE PATIENTS. The Lancet. sept 1983;322(8352):741. doi:10.1016/S0140-6736(83)92278-X

29. Chen L, Del Sorbo L, Grieco DL, Shklar O, Junhasavasdikul D, Telias I, et al. Airway Closure in Acute Respiratory Distress Syndrome: An Underestimated and Misinterpreted Phenomenon. Am J Respir Crit Care Med. 1 janv 2018;197(1):132-6. doi:10.1164/rccm.201702-0388LE

30. Chen L, Del Sorbo L, Grieco DL, Junhasavasdikul D, Rittayamai N, Soliman I, et al. Potential for Lung Recruitment Estimated by the Recruitment-to-Inflation Ratio in Acute Respiratory Distress

Syndrome. A Clinical Trial. Am J Respir Crit Care Med. 15 janv 2020;201(2):178-87. doi:10.1164/rccm.201902-0334OC

31. D'Alto M, Marra AM, Severino S, Salzano A, Romeo E, De Rosa R, et al. Right ventricular-arterial uncoupling independently predicts survival in COVID-19 ARDS. Crit Care. déc 2020;24(1):670. doi:10.1186/s13054-020-03385-5

32. Todaro MC, Carerj S, Zito C, Trifirò MP, Consolo G, Khandheria B. Echocardiographic evaluation of right ventricular-arterial coupling in pulmonary hypertension. Am J Cardiovasc Dis. 2020;10(4):272-83. PubMed PMID: 33224574; PubMed Central PMCID: PMC7675169.

33. Tello K, Axmann J, Ghofrani HA, Naeije R, Narcin N, Rieth A, et al. Relevance of the TAPSE/PASP ratio in pulmonary arterial hypertension. International Journal of Cardiology. sept 2018;266:229-35. doi:10.1016/j.ijcard.2018.01.053

34. Costa ELV, Borges JB, Melo A, Suarez-Sipmann F, Toufen C, Bohm SH, et al. Bedside estimation of recruitable alveolar collapse and hyperdistension by electrical impedance tomography. Intensive Care Med. juin 2009;35(6):1132-7. doi:10.1007/s00134-009-1447-y

35. Borges JB, Suarez-Sipmann F, Bohm SH, Tusman G, Melo A, Maripuu E, et al. Regional lung perfusion estimated by electrical impedance tomography in a piglet model of lung collapse. Journal of Applied Physiology. 1 janv 2012;112(1):225-36. doi:10.1152/japplphysiol.01090.2010

36. Perier F, Tuffet S, Maraffi T, Alcala G, Victor M, Haudebourg AF, et al. Effect of Positive End-Expiratory Pressure and Proning on Ventilation and Perfusion in COVID-19 Acute Respiratory Distress Syndrome. Am J Respir Crit Care Med. 15 déc 2020;202(12):1713-7. doi:10.1164/rccm.202008-3058LE

37. Pavlovsky B, Pesenti A, Spinelli E, Scaramuzzo G, Marongiu I, Tagliabue P, et al. Effects of PEEP on regional ventilation-perfusion mismatch in the acute respiratory distress syndrome. Crit Care. déc 2022;26(1):211. doi:10.1186/s13054-022-04085-y

38. Rezoagli E, Bastia L, Grassi A, Chieregato A, Langer T, Grasselli G, et al. Paradoxical Effect of Chest Wall Compression on Respiratory System Compliance. Chest. oct 2021;160(4):1335-9. doi:10.1016/j.chest.2021.05.057

39. Bastia L, Rezoagli E, Guarnieri M, Engelberts D, Forlini C, Marrazzo F, et al. External chest-wall compression in prolonged COVID-19 ARDS with low-compliance: a physiological study. Ann Intensive Care. déc 2022;12(1):35. doi:10.1186/s13613-022-01008-6

40. Jardin F, Delorme G, Hardy A, Auvert B, Beauchet A, Bourdarias JP. Reevaluation of Hemodynamic Consequences of Positive Pressure Ventilation: Emphasis on Cyclic Right Ventricular Afterloading by Mechanical Lung Inflation. Anesthesiology. 1 juin 1990;72(6):966-70. doi:10.1097/00000542-199006000-00003

41. Vieillard-Baron A, Loubieres Y, Schmitt JM, Page B, Dubourg O, Jardin F. Cyclic changes in right ventricular output impedance during mechanical ventilation. Journal of Applied Physiology. 1 nov 1999;87(5):1644-50. doi:10.1152/jappl.1999.87.5.1644

42. Zapol WM, Snider MT. Pulmonary Hypertension in Severe Acute Respiratory Failure. N Engl J Med. 3 mars 1977;296(9):476-80. doi:10.1056/NEJM197703032960903

43. Vieillard-Baron A, Schmitt JM, Augarde R, Fellahi JL, Prin S, Page B, et al. Acute cor pulmonale in acute respiratory distress syndrome submitted to protective ventilation: Incidence, clinical

implications, and prognosis: Critical Care Medicine. août 2001;29(8):1551-5. doi:10.1097/00003246-200108000-00009

44. Schmitt JM, Vieillard-Baron A, Augarde R, Prin S, Page B, Jardin F. Positive end-expiratory pressure titration in acute respiratory distress syndrome patients: Impact on right ventricular outflow impedance evaluated by pulmonary artery Doppler flow velocity measurements: Critical Care Medicine. juin 2001;29(6):1154-8. doi:10.1097/00003246-200106000-00012

45. Berger D, Moller PW, Weber A, Bloch A, Bloechlinger S, Haenggi M, et al. Effect of PEEP, blood volume, and inspiratory hold maneuvers on venous return. American Journal of Physiology-Heart and Circulatory Physiology. 1 sept 2016;311(3):H794-806. doi:10.1152/ajpheart.00931.2015

46. Tusman G, Gogniat E, Madorno M, Otero P, Dianti J, Ceballos IF, et al. Effect of PEEP on Dead Space in an Experimental Model of ARDS. Respiratory Care. 1 janv 2020;65(1):11-20. doi:10.4187/respcare.06843

47. Coffey RL, Albert RK, Robertson HT. Mechanisms of physiological dead space response to PEEP after acute oleic acid lung injury. Journal of Applied Physiology. 1 nov 1983;55(5):1550-7. doi:10.1152/jappl.1983.55.5.1550

48. Lassola S, Miori S, Sanna A, Pace R, Magnoni S, Vetrugno L, et al. Effect of chest wall loading during supine and prone position in a critically ill covid-19 patient: a new strategy for ARDS? Crit Care. déc 2021;25(1):442. doi:10.1186/s13054-021-03865-2

49. Fossali T, Pavlovsky B, Ottolina D, Colombo R, Basile MC, Castelli A, et al. Effects of Prone Position on Lung Recruitment and Ventilation-Perfusion Matching in Patients With COVID-19

Acute Respiratory Distress Syndrome: A Combined CT Scan/Electrical Impedance Tomography Study*. Critical Care Medicine. mai 2022;50(5):723-32. doi:10.1097/CCM.0000000000005450

50. Tuffet S, Maraffi T, Lacheny M, Perier F, Haudebourg AF, Boujelben MA, et al. Impact of cardiac output and alveolar ventilation in estimating ventilation/perfusion mismatch in ARDS using electrical impedance tomography. Crit Care. 8 mai 2023;27(1):176. doi:10.1186/s13054-023-04467-w

51. Larrabee S, Nugen S, Bruhn A, Porter I, Stowe S, Adler A, et al. Three-dimensional electrical impedance tomography to study regional ventilation/perfusion ratios in anesthetized pigs. American Journal of Physiology-Lung Cellular and Molecular Physiology. 1 nov 2023;325(5):L638-46. doi:10.1152/ajplung.00180.2023

Tables

Table 1: Patients characteristics at baseline

	All patients (n=20)	Responders (n=11)	Non responders (n=9)
Age (years)	68 (57; 74)	64 (56; 75)	70 (53; 73)
Sex. male. n (%)	16 (80)	8 (80)	8 (80)
BMI ($Kg.m^{-2}$)	26 (23; 31)	26 (22; 32)	26 (24; 32)
Tobacco use n (%)	5 (25)	1 (9)	4 (44)
Cardiac failure n (%)	1 (5)	0	1 (10)
Immunodepression n (%)	10 (50)	3 (30)	7 (70)
Clinical frailty scale	2.5 (2; 4)	2 (2; 4)	3 (2; 4)
SAPS 2	44 (28; 60)	36 (27; 54)	45 (25; 68)
SOFA	7 (5; 9)	7 (4; 9)	8 (5.5; 9)
MV duration before inclusion. days	1 (1; 1.25)	1 (0; 1)	1 (1; 2)
Aetiology of ARDS			
Bacterial pneumonia. n (%)	12 (60)	8 (73)	4 (44)
Aspiration pneumonia. n (%)	3 (15)	2 (18)	1 (11)
Fungal pneumonia. n (%)	2 (10)	0	2 (22)
Ventilatory settings at inclusion			
Tidal volume (mL.kg-1 PBW)	6 (5.8; 6.5)	6.2 (5.8; 6.6)	5.9 (5.7; 6.3)
P_{plat}, (cmH_2O)	28 (25; 29)	28 (26; 29)	28 (25; 30)
Total PEEP (cmH_2O)	15 (13; 17)	15 (12; 16)	15 (13; 17)
Driving pressure	13 (10; 14)	13 (10; 14)	13 (9; 15)
Crs ($ml.cmH_2O^{-1}$)	32.3 (26.4; 40)	32 (24; 40)	36 (26; 45)
VR	1.6 (1; 2.3)	1.7 (1.5; 2.3)	1.6 (1.4; 2.1)
Presence of AOP (%)	9 (45)	**3 (27)**	**6 (67)***
R/I ratio	0.46 (0.3; 0.85)	**0.33 (0.2; 0.67)**	**0.88 (0.46; 0.95)***
P/F (mmHg)	135 (107; 181)	148 (104; 175)	126 (106; 197)
PaCO2 (mmHg)	42 (39; 48)	42 (39.6; 48)	42.5 (36.5; 49)
Pronostic outcomes			
MV duration. days	14 (6; 20)	14 (3; 19)	13 (7.5; 22)
ICU Lengh of stay. days	22 (10; 31)	21 (10; 31)	22 (13; 29)
Mortality at day 28 n (%)	5 (25)	3 (27)	2 (22)

* p value (Mann–Whitney test) < 0.05 between responders and nonresponders

Abbreviations: BMI : body mass index, SAPS 2: Simplified Acute Physiology Score 2, SOFA : Sepsis-related Organ Failure Assessment, MV : mechanical ventilation, PBW: predicted body weight, PEEP: positive end expiratory pressure, Crs : respiratory system compliance computed as : tidal volume/ driving pressure, VR : ventilatory ratio computed as :[minute ventilation (ml/min) × PaCO2 (mm Hg)]/(predicted body weight × 100 × 37.5) , AOP: airway opening pressure, R/I : recruitment to inflation ratio(30)*, P/F : PaO_2 on FiO_2 ratio, ICU : intensive care unit*

Table 2: Hemodynamics, respiratory mechanics and gas exchanges

	All patients (n=20)		**Responders (n=11)**		**Nonresponders (n=9)**	
	Baseline	CACC	Baseline	CACC	Baseline	CACC
HR (min^{-1})	82 (68 ; 98)	80 (69 ; 95)	80 (66; 98)	79 (67;95)	83 (67; 100)	82 (66.5; 105)
SpO2 (%)	97 (96 ; 98)	96 (95 ; 98)	97 (96; 98)	97 (96;98)	96 (95; 98)	95 (92.5; 99)
SBP (mmHg)	116 (106 ; 124)	116 (108 ; 134)	117 (106; 122)	114 (92;127)	115 (107; 134)	121 (111; 137.5)
DBP (mmHg)	**57 (50 ; 63)**	**59 (54 ; 70) †**	**56 (49; 61)**	**59 (56; 68)†**	59 (48; 64)	59 (50; 73)
MBP (mmHg)	**74 (69 ; 84)**	**78 (71 ; 92) †**	74 (68; 79)	76 (75; 87)	76 (68; 87)	81 (69; 93)
CVP (mmHg)	15 (10 ; 18)	14 (10 ; 18)	14 (9; 18)	13 (9;16)	15 (13; 18)	14 (12; 21)
Norepinephrine (mg/h)	0.4 (0 ; 1.7)	0.5 (0 ; 1.9)	0.4 (0 ; 2.1)	0.2 (0 ; 1.4)	1 (0.05; 2.5)	1.3 (0.05; 2.7)
Respiratory mechanics						
Vte (ml)	414 (355 ; 428)	418 (361 ; 445)	415 (340; 420)	411 (342;438)	392 (364; 467)	441 (370; 455)
Ppeak (cmH_2O)	40 (38 ; 44)	40 (37 ; 45)	40 (37; 41)	39 (35;40)	40 (38; 48)	43 (38; 50)
Pplat (cmH_2O)	28 (25 ; 29)	27 (25 ; 29)	**28 (26; 29)**	**25 (24;27)†**	**28 (25; 30)**	**29 (26; 31)†**
Peep t (cmH_2O)	15 (13 ; 17)	15 (13 ; 17)	15 (12; 16)	15 (13;18)	15 (13; 17)	15 (14; 17)
Cp RS (ml/cmH_2O)	**32 (26 ; 40)**	**36 (28 ; 49) †**	**32 (24; 40)**	**38 (31;49)†**	36 (26; 45)	28 (25; 48)
DP (cmH2O)	13 (10 ; 14)	12 (8.8 ; 15)	**13 (10; 14)**	**10 (8;12)†**	**13 (9; 15)**	**15 (9; 17)†**
Arterial and venous blood gas						
PH	7.3 (7.3 ; 7.4)	7.3 (7.3 ; 7.4)	7.3 (7.3; 7.4)	7.4 (7.3;7.4)	7.3 (7.2; 7.4)	7.3 (7.2; 7.4)
PaO_2 (mmHg)	80 (75 ; 89)	79 (63 ; 86)	**85 (79; 102)**	80 (63;93)	**75 (67; 82)***	68 (61; 84)
$PaCO_2$ (mmHg)	42 (39 ; 48)	42 (37 ; 45)	42 (40; 48)	41 (36;45)	43 (36; 49)	43 (37.5; 47)
Lactate	1.1 (0.9 ; 1.7)	1.3 (1 ; 1.6)	**1.6 (1.1; 2)**	1.6 (1.3;1.9)	**0.9 (0.8; 1.2)***	1 (0.8; 1.4)
PaO_2/FiO_2	**135 (107 ; 181)**	**120 (94 ; 168) †**	158 (106; 184)	124 (107;173)	**117 (101; 181)**	**95 (79; 145)†**
$ScvO_2$ (%)	68 (65 ; 76)	74 (63 ; 80)	70 (64; 79)	73 (67;81)	66 (65; 75)	75 (58; 79)

**p value (Mann–Whitney test) < 0.05 between responders and nonresponders; †p value (Wilcoxon paired test) < 0.05 between baseline and CACC.*

Abbreviations: HR: heart rate, SBP : systolic blood pressure, DBP : diastolic blood pressure, MBP : mean blood pressure, CVP : central venous pressure, Ppeak : peak airway pressure, Pplat : plateau pressure, Peept : total positive end expiratory pressure, Cp RS : compliance respiratory system, DP : driving pressure, PaO_2 : arterial oxygen pressure, $PaCO_2$: arterial carbon dioxid, $ScvO_2$: central oxygen venous saturation

Table 3 Echocardiographic parameters

	All patients (n=20)		Responders (=11)		Nonresponders (=9)	
	Baseline	*CACC*	*Baseline*	*CACC*	*Baseline*	*CACC*
Left ventricle assessment						
LVEF, %	60 (53; 64)	60 (53; 64)	60 (50-60)	60 (50-60)	60 (60-68)	60 (60-70)
E velocity, m/s	67 (58; 82)	71 (58; 87)	64 (51-79)	66 (54-72)	72 (64-88)	82 (71-108)
A velocity, m/s	69 (53; 89)	68 (48; 94)	63 (39-80)	49 (44-80)	81 (70-97)	87 (68-117)
Deceleration time, ms	240 (193; 330)	235 (191; 273)	245 (196-308)	234 (201-259)	217 (177-334)	239 (179-320)
Lateral e' velocity, cm/s	9 (6; 11)	9 (7; 10)	9 (6-11)	9.5 (6.3-11)	9 (5.8-11)	9 (6.5-10)
Lateral S' velocity, cm/s	9 (6.3; 11)	10 (6.8; 11)	7.7 (6-11)	11 (7-13)	10 (7-12)	9 (5.3-11)
E/A ratio	1 (0.81; 1.3)	1.1 (0.77; 1.3)	1.1 (0.96-1.3)	1.1 (0.82-1.4)	0.89 (0.8-1.2)	0.96 (0.71-1.2)
E/Lateral e'	8.8 (5.6; 13)	8.9 (6.9; 12)	8.8 (5-14)	6.9 (5.4-10)	9.1 (7.2-12)	12 (8.2-13)
LVOT VTI, cm	22 (13; 26)	22 (15; 26)	21 (12-25)	20 (15-23)	26 (19-28)	24 (19-28)
CO, l/min	5.8 (3.9; 6.8)	5.7 (4.6; 6.4)	5.2 (3.3-6.3)	5.2 (4-6.3)	6 (4.9-7)	6.5 (5.7-7.3)
Right ventricle assessment						
TAPSE (mm)	20 (15; 25)	22 (16; 24)	18 (15-24)	23 (15-24)	22 (15-27)	21 (16-27)
Tricuspid S' velocity, m/s	12 (12; 16)	14 (11; 16)	13 (10-16)	15 (12-16)	12 (12-16)	14 (10-17)
RV FAC, %	51 (45; 57)	53 (47; 57)	52 (47-60)	52 (45-56)	50 (41-56)	53 (48-59)
RV/LV ratio	0.7 (0.66; 0.9)	0.7 (0.61; 0.8)	0.7 (0.7-0.9)	0.7 (0.68-0.8)	0.7 (0.63-0.9)	0.7 (0.6-0.85)
sLV eccentricity index	1 (0.95; 1.2)	1.1 (0.9; 1.2)	1 (0.82; 1.1)	1.1 (0.88; 1.2)	1.2 (1; 1.2)	1.2 (0.9; 1.3)
ACP, n (%)	4 (20)	4 (20)	2 (10)	3 (15)	2 (10)	1 (5)
RVOT acceleration time, ms	95 (88; 115)	97 (86; 113)	95 (90-126)	102 (95-120)	87 (67-111)	86 (68-96)
RVOT VTI, cm	17 (12; 20)	16 (13; 19)	14 (11-21)	15 (12-21)	17 (14-19)	16 (14-17)
TRV, m/sec	**2.6 (2.5; 2.9)**	**2.5 (2.1; 2.7)†**	**2.7 (2.4-2.9)**	**2.4 (2-2.6) †**	2.7 (2.4-2.9)	2.7 (2.3-2.8)
TR pressure gradient (mmHg)	**28 (25; 34)**	**25 (18; 29) †**	**29 (23-35)**	**21 (18-29) †**	29 (24-34)	30 (21-32)
RVSP (mmHg)	**38 (35; 45)**	**36 (32; 42) †**	**40 (36-43)**	**36 (30-40) †**	37 (35-49)	42 (35-50)
RV-PA coupling						
TAPSE/RVSP (mm/mmHg)	**0.46 (0.33; 0.59)**	**0.55 (0.39; 0.64)†**	**0.42 (0.36; 0.63)**	**0.57 (0.43; 0.66)†**	0.58 (0.46; 0.74)	0.57 (0.34; 0.63)

† p< 0,05 difference CACC vs baseline, by Wilcoxon paired tests. Abbreviations : LVEF : left ventricular ejection fraction, LVOT VTI : left ventricle outflow tract velocity time integral, CO : cardiac output, TAPSE: tricuspid annular plane systolic excursion, S' wave tricuspid annular systolic velocity, RVFAC : right ventricle fractional area change, RV/LV : right ventricle end-diastolic to LV end-diastolic diameter ratio, sLV eccentricity index : systolic left ventricle eccentricity index; ACP : Acute cor pulmonale was defined as the presence of paradoxical septal motion (PSM) and RV end-diastolic to LV end-diastolic diameter ratio > 0.6, sPAP, RVOT acceleration time : right ventricle

outflow track acceleration time, RVOT VTI : right ventricle outflow track velocity time integral, TRV : Tricuspid regurgitation velocity, TR : tricuspid regurgitation, RVSP : right ventricle systolic pressure.

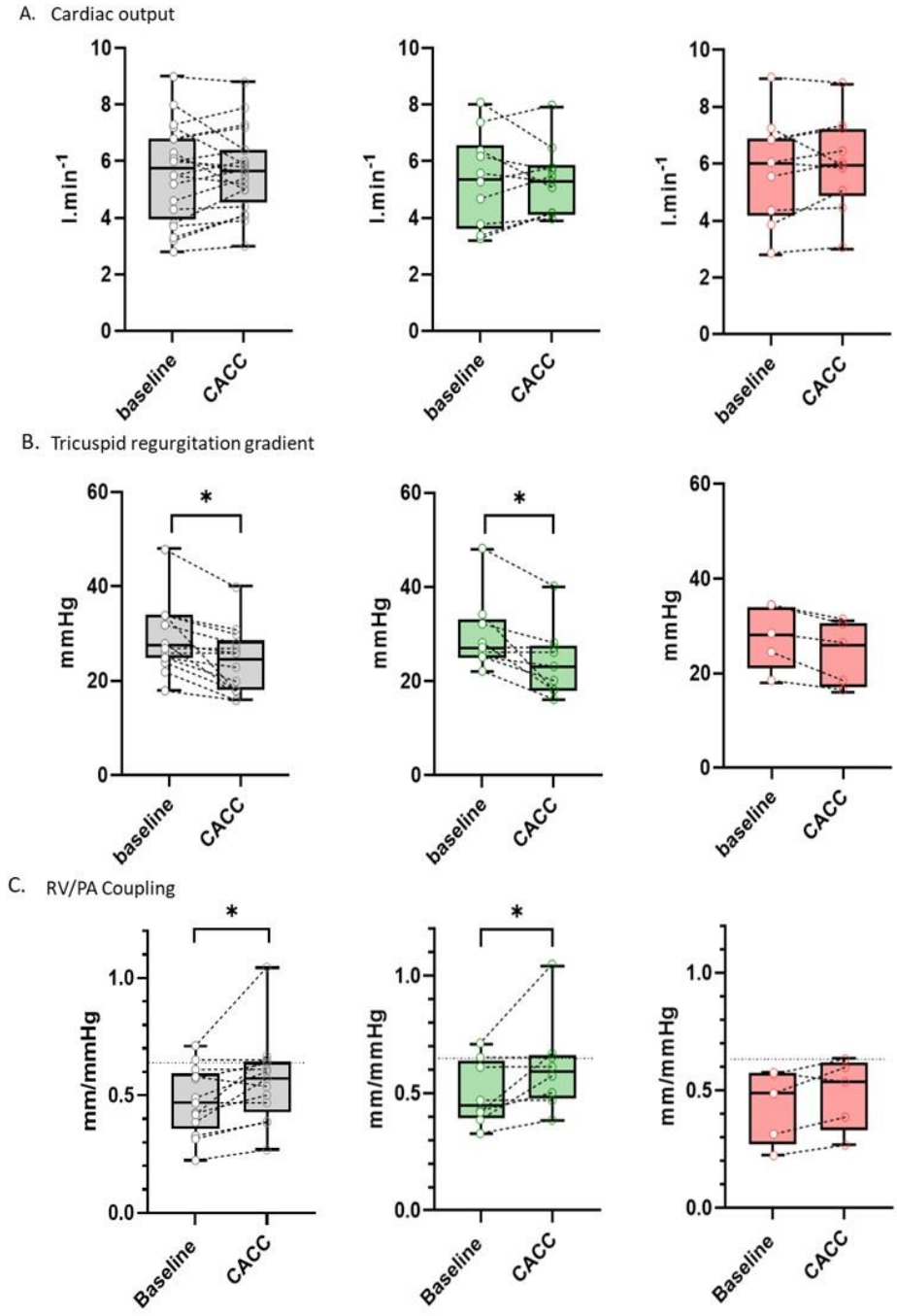
Table 4: Ventilation and perfusion distributions

	All patients (n=20)		Responders (n=11)		Nonresponders (n=9)	
	Baseline	*CACC*	*Baseline*	*CACC*	*Baseline*	*CACC*
Ventilation distribution						
Anterior distribution, %	**47 (40 ; 57)**	**50 (44 ; 59) †**	**46 (39; 57)**	**51 (45; 64)†**	50 (40; 56)	49 (43; 56)
Anterior compliance (ml/cmH_2O)	**14.8 (11.8 ; 18.2)**	**17.4 (13.9 ; 21.8) †**	**15 (10,5; 17,1)**	**20 (16,8; 23)†**	15 (13; 20)	14 (12; 18)
Posterior compliance (ml/cmH2O)	17.3 (11.8 ; 23.3)	17.5 (13.2 ; 23.1)	**17 (11,8; 24,1)**	**19 (13,2; 26,9)†**	19 (13; 23)	17 (12; 21)
GI	0.52 (0.49 ; 0.54)	0.51 (0.49 ; 0.54)	0,53 (0,48; 0,55)	0,51 (0,49; 0,54)	0.51 (0.5; 0.53)	0.5 (0.49; 0.55)
COV	0.52 (0.50 ; 0.53)	0.52 (0.50 ; 0.53)	**0.52 (0,5; 0,55)**	**0.51 (0,5; 0,52)†**	0.51 (0.5; 0.55)	0.52 (0.5; 0.53)
EELI variation, AU	-	**-28 (-39 ; -21) †**	-	**-26 (-43; -22)†**	-	**-34 (-38; -167) †**
EELV variation, ml	-	**-683 (-832 ; -506) †**	-	**-658 (-831; -500)†**	-	**-704 (-856; -405) †**
Overdistension (%)			**30 (23; 50)**		**13 (7; 21)***	
Collapse (%)			0,3 (0; 1,5)		0.7 (0.3; 4)	
Perfusion distribution						
Anterior distribution, %	44 (30 ; 5)	44 (38 ; 5)	40 (28; 46)	47 (39; 50)	48 (31; 0.51)	43 (35; 48)
Ventilation distribution to V/Q ratio (%)						
V' to low V/Q	0,38 (0; 1,9)	1,8 (0,023; 3,7)	0.9 (0; 2)	0.8 (0; 2)	0,33 (0; 1,4)	2,9 (0,068; 5,3)
V' to normal V/Q	62 (33; 80)	53 (33; 74)	62 (34; 75)	56 (43; 74)	60 (16; 90)	39 (22; 77)
V' to high V/Q	25 (8,9; 48)	27 (13; 53)	24 (9.3; 40)	28 (16; 54)	33 (3,5; 82)	9 (5,6; 57)
V' to dead space V/Q	5 (2,2; 17)	7 (3.3 ; 12)	**12 (4; 23)**	6 (3; 12)	**2 (2; 6)***	8 (5; 13)
Wasted ventilation	29 (12 ; 33)	29 (21 ; 33)	**32 (25; 46)**	31 (23; 37)	**16 (12 ; 30)***	25 (15 ; 34)
Perfusion distribution to V/Q ratio (%)						
Q to shunt V/Q	**3 (1,6; 5,4)**	**6 (3; 9)†**	3 (1.8; 8.2)	8 (1.4; 10)	**2 (1; 4)**	**5 (3; 8)†**
Q to low V/Q	1,1 (0; 5,3)	6,5 (0,39; 9,8)	2 (0; 7.9)	3 (0; 8.4)	1 (0; 4)	7 (0.3; 18)
Q to normal V/Q	81 (42; 90)	71 (51; 84)	80 (53; 88)	70 (53; 84)	87 (64.5; 94)	81 (63; 85)
Q to high V/Q	9,9 (2,9; 31)	8,9 (3,6; 33)	13 (4.4; 27)	8 (6.4; 33)	10 (1.6; 29)	10 (2; 16)
Wasted perfusion	11 (6 ; 15)	12 (7 ; 15)	12 (6; 16)	13 (7; 15)	**8 (4; 12)**	**10 (7; 18)†**

*p value (Mann–Whitney test) < 0.05 between responders and nonresponders at baseline; †p value (Wilcoxon paired test) < 0.05 between baseline and CACC.
Abbreviations: GI: global inhomogeneity, COV : center of ventilation, EELZ : end expiratory lung impedance, EELV : end expiratory lung volume, V' : ventilation, V/Q : ventilation/perfusion ratio

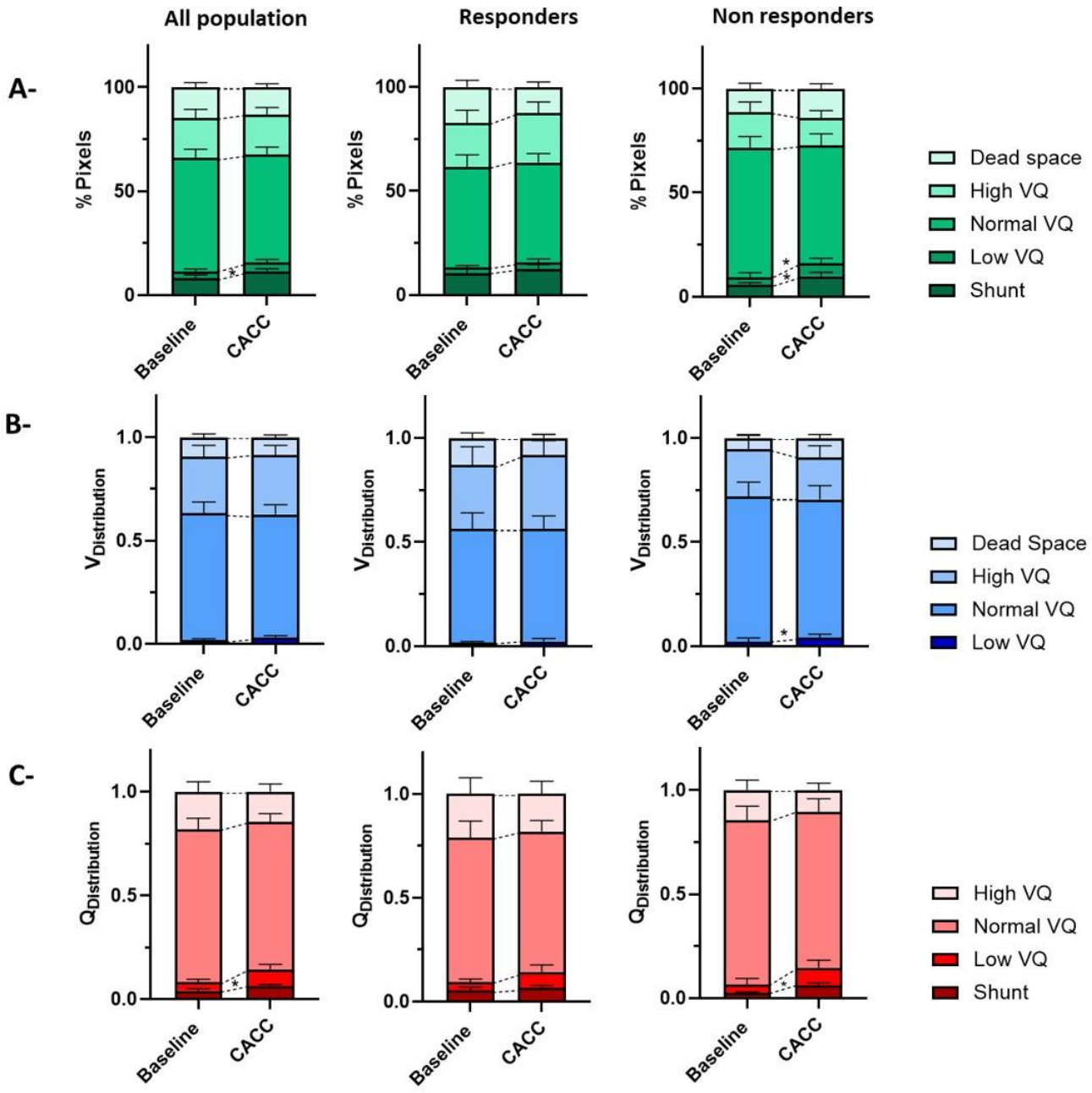
Figures:

Figure 1. Hemodynamic effects of CACC. Total population is in grey, responders in green and nonresponders in red



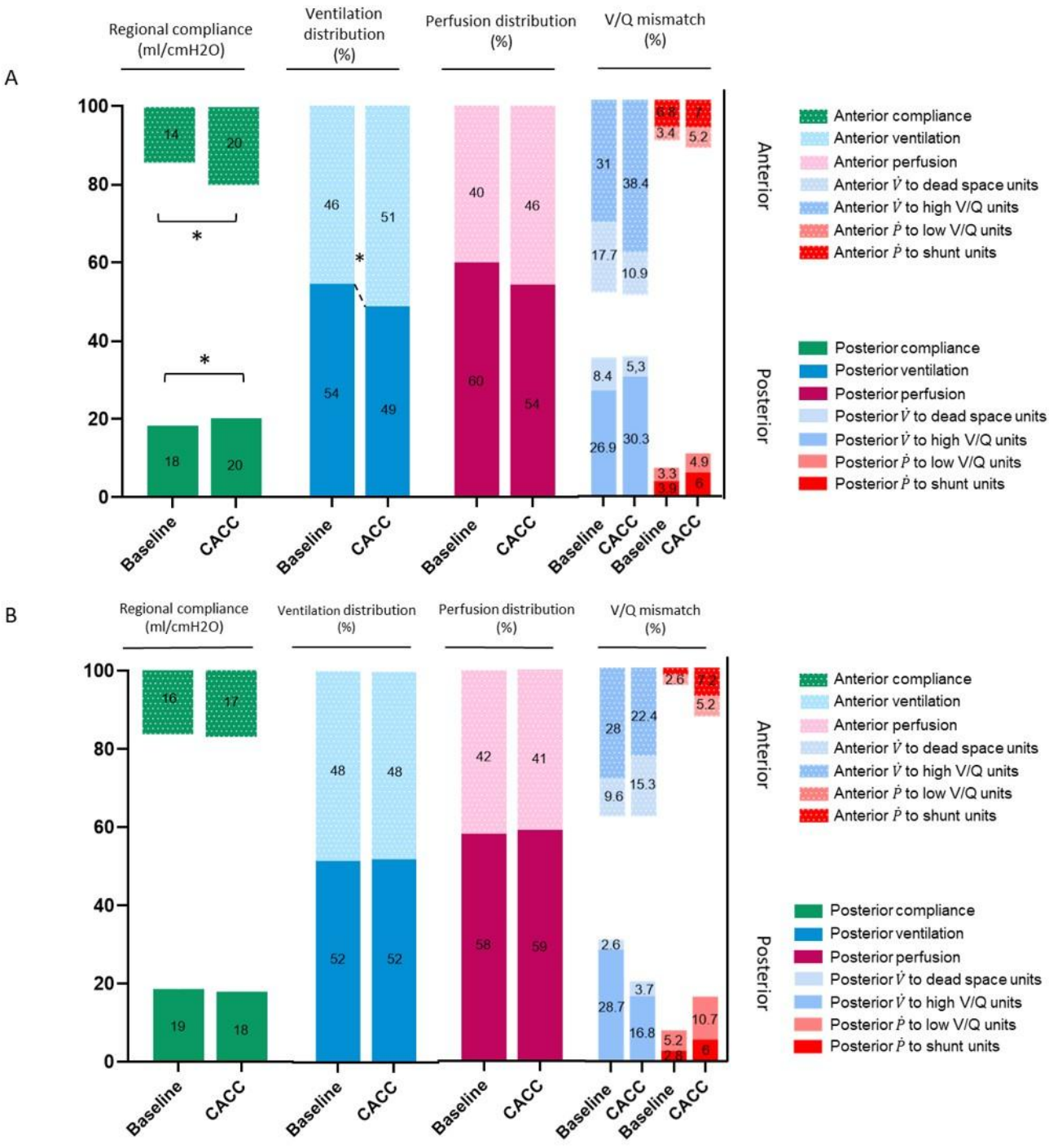
A: cardiac output, calculated as LVOT area X LVOT VTI X heart rate. B. Tricuspid regurgitation gradient. C. Right Ventricle / Pulmonary Artery (RV/PA) coupling assessed by the TAPSE/RVSP ratio. The horizontal dotted line represents the threshold associated with worse outcomes (0.625 mm/mmHg) (31)

Figure 2: Distribution of Ventilation and Perfusion according to their V/Q classes



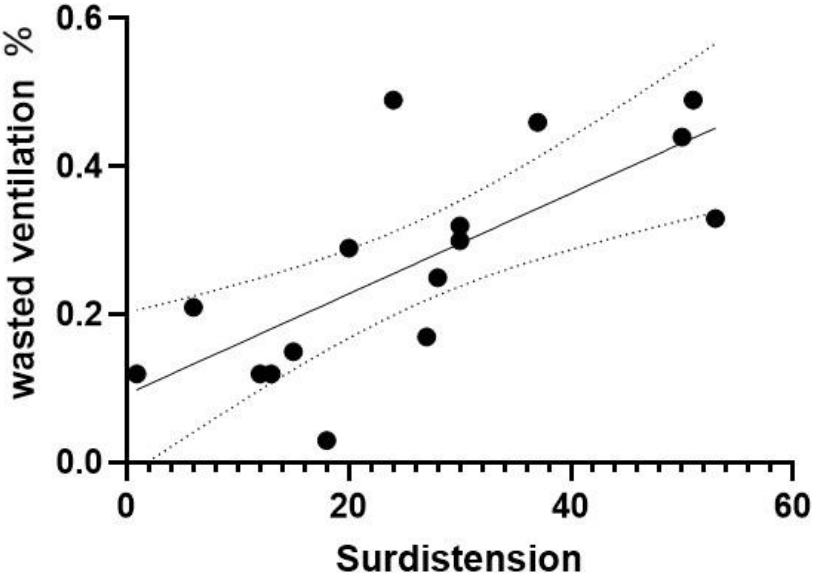
Distribution of (A) the number of pixels (green bars), (B) ventilation ($V_{Distribution}$, blue bars) and (C) perfusion ($Q_{Distribution}$, red bars) across the different ranges of V/Q ratio ranges in the entire population, responders and nonresponders. Histograms represent mean values (± SEM). *$p < 0.05$ by paired Wilcoxon test

Figure 3: Regional compliance, ventilation, perfusion distribution and V/Q mismatch at Baseline and during CACC, in responders (A) and nonresponders (B).



Regionnal compliance, ventilation, perfusion distribution and V/Q mismatch at Baseline and during CACC, in responders (A) and nonresponders (B). For better illustration, data are shown as mean (not median) values. *p < 0.05 by paired Wilcoxon test

Figure 4: Correlation between Overdistension and wasted ventilation at baseline



ONLINE DATA SUPPLEMENT

ADDITIONAL METHODS

Echocardiographic measurements:

- *Left ventricle:* left ventricular ejection fraction (LVEF), LV outflow tract (LVOT) and the velocity time integral (VTI), transmitral E and A velocity using doppler. Tissue Doppler imaging was performed to measure systolic (S'), early (e'), and late (a') diastolic peak myocardial velocities at the lateral mitral annulus. Cardiac output (CO) was calculated as follows: LVOT area X LVOT VTI X heart rate.
- *Right ventricle:* ventricular tricuspid annular plane systolic excursion (TAPSE), S' wave tricuspid annular systolic velocity, right ventricle fractional area change (RV FAC), right ventricle end-diastolic to LV end-diastolic diameter ratio, systolic left ventricle eccentricity index, presence of paradoxical septal motion (PSM). Acute cor pulmonale was defined as the presence of paradoxical septal motion (PSM) and RV end-diastolic diameter to LV end-diastolic diameter ratio > 0.6. RV outflow track acceleration time, right ventricle outflow track velocity time integral (RVOT VTI), tricuspid regurgitation velocity (TRV), tricuspid regurgitation gradient (TR). Right ventricle systolic pressure (RVSP) was estimated by adding estimated right atrial pressure to tricuspid regurgitation gradient, estimated pulmonary vascular resistance was estimated as : flow tricuspid regurgitation (TR) Vmax (m/s)/ RVOT VTI(1). TAPSE/RVSP was chosen as a noninvasive surrogate of RV-pulmonary artery coupling as previously described (2–4).

Electrical Impedance Tomography analysis

Perfusion method:
Lung perfusion was estimated by injecting a 10-ml bolus of 7.5% hypertonic saline into a central venous jugular catheter during a 10 to 20 secondes apnea using the mean airway pressure (measured in the ventilator before the apnea). Perfusion distribution was measured using the maximal slope of each pixel with a first-pass dilution kinetic model(5,6).

Lung contouring method:
Ventilation and perfusion maps were reconstructed offline with dedicated LabVIEW software.

A pixel i was considered ventilated if it received a fraction greater than 10% of the maximum ventilated (Pixel $_{refV}$). A pixel i was considered perfused if it received a fraction greater than 10% of the maximum perfused pixel (Pixel $_{refP}$).

Global and Regional analysis of V/Q mismatch:

Cardiac output (Qc) was measured using echocardiography with the formula: Qc = LVOT (left ventricular outflow track) area X LVOT VTI (velocity time integral) X heart rate.

Alveolar ventilation (VA) was calculated as 70% of the expiratory minute ventilation measured on the mechanical ventilator(7,8).

Absolute V/Q pixelwise were calculated as the division between : the proportion of total ventilation through one pixel i (V%,i) multiplied by the total alveolar ventilation, and the proportion of total perfusion through one pixel i (Q%,i) multiplied by the cardiac output (7,8) .

$$\left(\frac{\mathrm{V}}{\mathrm{Q}}\right)_{\mathrm{Abs,i}} = \frac{\mathrm{V_{\%,i}} * V_A}{\mathrm{Q_{\%,i}} * Q_c}$$

According to their V/Q ratio, pixels have been classified among five different classes: shunt pixels (V/Q ratio <0.1); pixels with low V/Q ratio (V/Q ratio 0.1–0.5); pixels with normal V/Q ratio (V/Q ratio 0.5–2); pixels with high V/Q ratio (V/Q ratio 2–10); dead space pixels (V/Q ratio >10).

We also calculated:

- Wasted ventilation (9) : $= \sum_{i=1}^{n} \left(\log \left(\frac{\dot{V}}{Q} \right)_i * Vt_i \right)$, where n is the number of pixels in the functional EIT image within each ROI, including only units with V/Q ratio >1
- Wasted perfusion (9) $= \sum_{i=1}^{n} \left(\log \left(\frac{\dot{V}}{Q} \right)_i * Q_i \right)$, where n is the number of pixels in the functional EIT image each ROI, including only units with V/Q ratio <1

ADDITIONAL RESULTS :

Table E 1. Regional distribution of ventilation, perfusion, and V/Q ratios.

	All patients (n=20)		**Responders (n=11)**		**Non-Responders (n=9)**	
	Baseline	*CACC*	*Baseline*	*CACC*	*Baseline*	*CACC*
Anterior zone						
Ventilation distribution to V/Q ratio (%)						
V' to low V/Q	0 (0; 0,68)	0,1 (0; 5,2)	0 (0; 0.7)	0 (0; 3.5)	0 (0; 0,64)	1,4 (0; 7,9)
V' to normal V/Q	54 (25; 79)	52 (31; 64)	53 (24; 79)	49 (45; 63)	43 (22; 81)	48 (24; 69)
V' to high V/Q	28 (11; 52)	34 (18; 48)	22 (17; 50)	39 (21; 49)	40 (5,1; 71)	34 (8,9; 56)
V' to dead space V/Q	6,2 (1,6; 27)	12 (3,6; 22)	11 (3.5; 32)	8.7 (3; 17)	**2,4 (0,63; 11) ***	16 (6,4; 23)
Perfusion distribution to V/Q ratio (%)						
Q to shunt V/Q	2,5 (0,53; 6,1)	4,1 (1; 13)	3.4 (1.6; 14)	3.4 (1; 14)	1,7 (0,3; 3,9)	4,7 (0,83; 19)
Q to low V/Q	0 (0; 0,2)	0 ,32 (0; 13)	0 (0; 3.8)	0 (0; 10)	0 (0; 1,9)	4,8 (0; 16)
Q to normal V/Q	73 (45; 86)	64 (37; 85)	74 (58; 79)	67 (53; 77)	66 (32; 97)	66 (35; 87)
Q to high V/Q	20 (6,1; 42)	18 (11; 34)	16 (7.5; 42)	0.2 (0.1; 0.36)	33 (2,7; 57)	22 (8,4; 39)
Posterior zone						
Ventilation distribution to V/Q ratio (%)						
V' to low V/Q	0,26 (0; 2,9)	0,61 (0; 4)	0.5 (0; 3)	0.4 (0; 2)	0 (0; 2.9)	4 (0; 13)
V' to normal V/Q	72 (11; 93)	73 (35; 86)	80 (15; 94)	71 (34; 84)	67 (48; 92)	77 (55; 90)
V' to high V/Q	20 (3,3; 78)	18 (4,3; 60)	9 (3.3; 46)	14 (5.9; 64)	31 (4.1; 40)	16 (0; 33)
V' to dead space V/Q	2,9 (1,1; 4,4)	3,5 (2,5; 6,5)	2.6 (1.2; 11)	4 (2.5; 8.4)	3 (0.9; 4)	3 (3; 5)
Perfusion distribution to V/Q ratio (%)						
Q to shunt V/Q	**1,7 (0,37; 5,3)**	**4 (11; 9,9) †**	2 (0.16; 5.8)	4 (2; 12)	1.5 (0.5; 6)	4 (1; 10)
Q to low V/Q	0,47 (0; 0,06)	1,3 (0; 9,3)	0.1 (0; 6.3)	0.4 (0; 4.9)	0 (0; 6)	7 (0; 25)
Q to normal V/Q	83 (39; 93)	70 (45; 86)	85 (40; 93)	73 (43; 88)	86 (71; 94)	78 (59; 91)
Q to high V/Q	10 (1,1; 36)	6,6 (2; 41)	4.9 (1; 39)	6 (2; 55)	13 (0.75; 23)	7.5 (0; 18)

*p value (Mann–Whitney test) < 0.05 between responders and nonresponders; †p value (Wilcoxon paired test) < 0.05 between baseline and CACC.
Abbreviations: CACC: continuous anterior chest compression, V' : ventilation, Q: perfusion, V/Q : ventilation/perfusion ratio

Table E2. Changes in regional and global EELZ and EELV from baseline to CACC in all patients, and stratified by response to CACC.

	All patients (n=20)	Responders (n=11)	Nonresponders (n=9)
Anterior EELI variation (AU)	**-18.6 (-28.21; -10.26)**	-21 (-27.3; -11.4)	-14.2 (-31.6; -17)
Posterior EELI variation (AU)	**-9.9 (-18.34; -2.52)°**	-147 (-18.6; -4)	-5.6 (-21.9; -1.2)
EELI variation (AU)	-26.3(-43; -21.9)	-27.65 (-50; -18.85)	-33.9 (-39.7; -19.2)
EELV variation (ml)	-683 (-884; -502)	-658 (-831; -500)	-704 (-856; -405)
EELV variation/PBW (ml/kg)	-10.4 (-13; -7)	-10.4 (-14.6; -7)	-10.8 (-12.7; -6)

° means p value (Mann–Whitney test) < 0.05 between anterior and posterior zone.
Abbreviations: CACC: continuous anterior chest compression, AU: arbitrary unit, PBW: predicted body weight, EELI: end expiratory lung impedance, EELV: end expiratory lung volume

Additional figures legend:

Figure E1: Distribution of regional ventilation (VDistribution , blue bars) and perfusion (QDistribution, red bars) across different ranges of V/Q ratio ranges in the entire population, responders and nonresponders. Histograms represent mean values (± SEM). *p < 0.05 by paired Wilcoxon test.

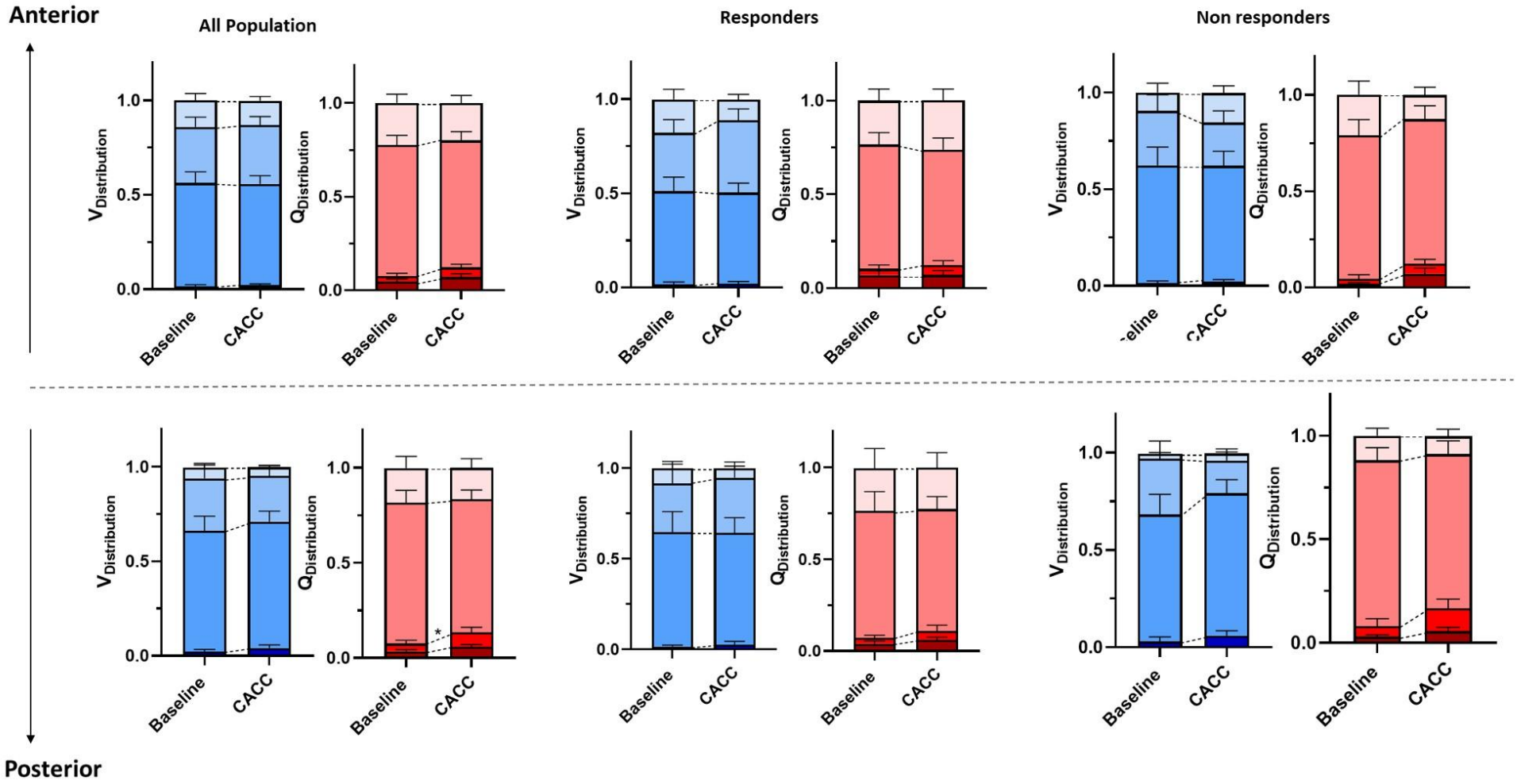
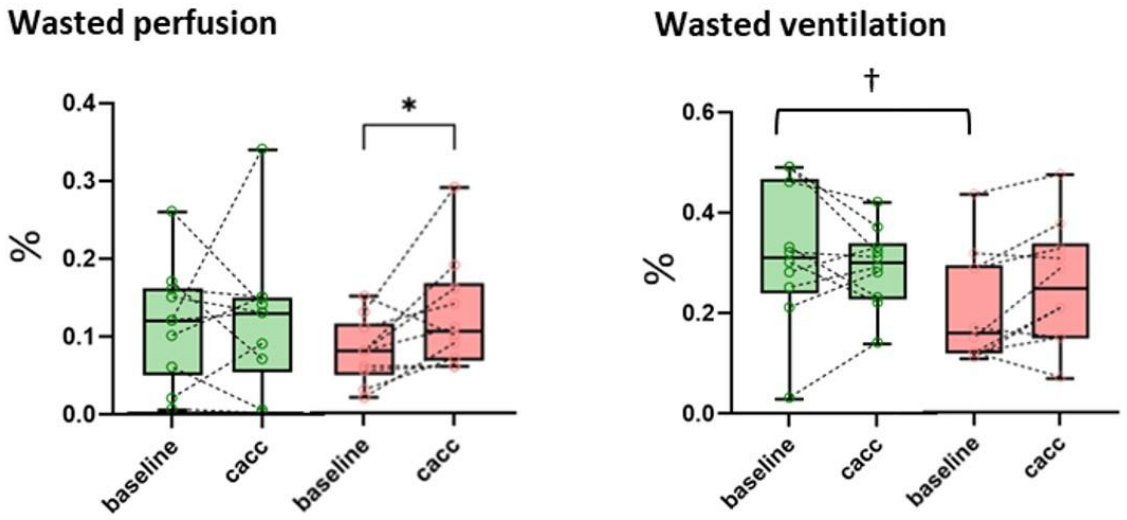

Anterior
All Population
Responders
Non responders
V Distribution
Q Distribution
1.0
0.5
0.0
Baseline
CACC
*
Posterior

Figure E2: Wasted perfusion and ventilation. Green boxes correspond to responders, red boxes are nonresponders. *p < 0.05 by paired Wilcoxon test, †p<0.05 by Mann–Whitney test



References :

1. Abbas AE, Franey LM, Marwick T, Maeder MT, Kaye DM, Vlahos AP, et al. Noninvasive Assessment of Pulmonary Vascular Resistance by Doppler Echocardiography. Journal of the American Society of Echocardiography. oct 2013;26(10):1170-7. doi:10.1016/j.echo.2013.06.003

2. D'Alto M, Marra AM, Severino S, Salzano A, Romeo E, De Rosa R, et al. Right ventricular-arterial uncoupling independently predicts survival in COVID-19 ARDS. Crit Care. déc 2020;24(1):670. doi:10.1186/s13054-020-03385-5

3. Todaro MC, Carerj S, Zito C, Trifirò MP, Consolo G, Khandheria B. Echocardiographic evaluation of right ventricular-arterial coupling in pulmonary hypertension. Am J Cardiovasc Dis. 2020;10(4):272-83. PubMed PMID: 33224574; PubMed Central PMCID: PMC7675169.

4. Tello K, Axmann J, Ghofrani HA, Naeije R, Narcin N, Rieth A, et al. Relevance of the TAPSE/PASP ratio in pulmonary arterial hypertension. International Journal of Cardiology. sept 2018;266:229-35. doi:10.1016/j.ijcard.2018.01.053

5. Borges JB, Suarez-Sipmann F, Bohm SH, Tusman G, Melo A, Maripuu E, et al. Regional lung perfusion estimated by electrical impedance tomography in a piglet model of lung collapse. Journal of Applied Physiology. 1 janv 2012;112(1):225-36. doi:10.1152/japplphysiol.01090.2010

6. Martin KT, Xin Y, Gaulton TG, Victor M, Santiago RR, Kim T, et al. Electrical Impedance Tomography Identifies Evolution of Regional Perfusion in a Porcine Model of Acute Respiratory Distress Syndrome. Anesthesiology. 1 déc 2023;139(6):815-26. doi:10.1097/ALN.0000000000004731

7. Tuffet S, Maraffi T, Lacheny M, Perier F, Haudebourg AF, Boujelben MA, et al. Impact of cardiac output and alveolar ventilation in estimating ventilation/perfusion mismatch in ARDS using electrical impedance tomography. Crit Care. 8 mai 2023;27(1):176. doi:10.1186/s13054-023-04467-w

8. Perier F, Tuffet S, Maraffi T, Alcala G, Victor M, Haudebourg AF, et al. Effect of Positive End-Expiratory Pressure and Proning on Ventilation and Perfusion in COVID-19 Acute Respiratory Distress Syndrome. Am J Respir Crit Care Med. 15 déc 2020;202(12):1713-7. doi:10.1164/rccm.202008-3058LE

9. Pavlovsky B, Pesenti A, Spinelli E, Scaramuzzo G, Marongiu I, Tagliabue P, et al. Effects of PEEP on regional ventilation-perfusion mismatch in the acute respiratory distress syndrome. Crit Care. déc 2022;26(1):211. doi:10.1186/s13054-022-04085-y